

Simulation and Modeling for Soft Recovery of p-i-n Rectifiers

Kartikeya Mayaram, Ben Tien, Chenming Hu, and Donald O. Pederson

Department of Electrical Engineering and Computer Sciences
 Electronics Research Laboratory
 University of California
 Berkeley, CA 94720

Abstract

Soft recovery of fast switching p-i-n rectifiers is studied using experimental data and a new coupled device and circuit simulator. An analytical model for determining lifetimes is presented and verified by numerical simulations. The softness factor is difficult to model analytically, hence simulations are necessary. Coupled device and circuit simulations also allow a determination of the magnitude of the inductive voltage spike that appears across the rectifier during an unclamped reverse recovery.

I. Coupled Device and Circuit Simulator: CODECS

CODECS is a coupled device and circuit simulator that allows accurate and detailed simulation of semiconductor circuits. The simulation environment of CODECS enables one to model critical devices within a circuit by numerical (physical) models based upon the solution of Poisson's equation and the current continuity equations. Analytical models can be used for the non-critical devices. CODECS incorporates SPICE3 for the circuit simulation capability and for analytical models of semiconductor devices. Numerical models are provided by a new one- and two-dimensional device simulator. Dc, transient, and small-signal ac analyses can be performed on circuits containing one and two-dimensional numerical models. The numerical models in CODECS include physical effects such as bandgap narrowing, Shockley-Hall-Read and Auger recombinations, concentration and field dependent mobilities, concentration dependent lifetimes, and avalanche generation

II. Simulation of Reverse Recovery

The turnoff under an inductive load is simulated using CODECS with the simple circuit shown in Fig. 1; the diode is idealized to have a piecewise-uniform doping profile. The source voltage

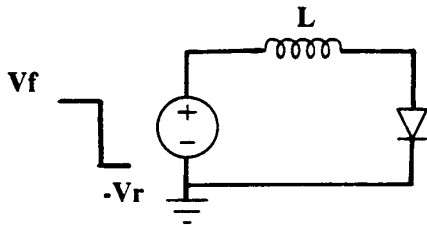


Figure 1: A simple circuit used for simulating reverse recovery is stepped from a positive voltage to a negative voltage. Simulated waveforms of the diode current and voltage are shown in

Fig. 2 for a diode with a $15\mu\text{m}$ wide i-region and a doping of 10^{14} cm^{-3} , and $V_R = 10\text{V}$. The carrier concentrations and electric fields corresponding to the time instants A – G in Fig. 2, are shown in Figs. 3 and 4, respectively. Initially the i-region

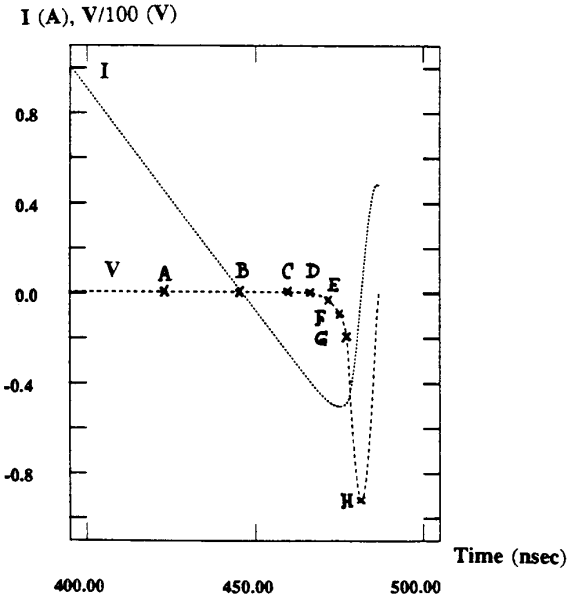


Figure 2: The simulated current and voltage waveforms during reverse recovery

is conductivity modulated because the diode is operating under high-level injection conditions. With time the carriers are removed by recombination and back-injection. At a certain time a depletion region starts forming at the p-i junction and the diode becomes blocking. Finally, the i-region is completely depleted of mobile carriers. The reverse recovery current peaks when a large portion of the $15\mu\text{m}$ i-region is depleted so that the rectifier voltage is equal to the reverse voltage of the source.

It is seen from Fig. 2 that the simulated current waveform is almost triangular in nature. Therefore, for modeling purposes, use will be made of the idealized triangular waveform shown in Fig. 5; different time instants are also shown. The softness factor is defined to be $S = T_B/T_A$.

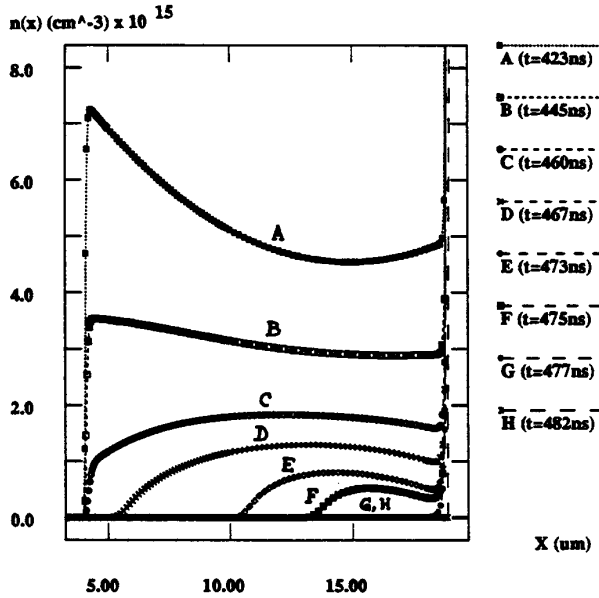


Figure 3: Electron concentrations as a function of time

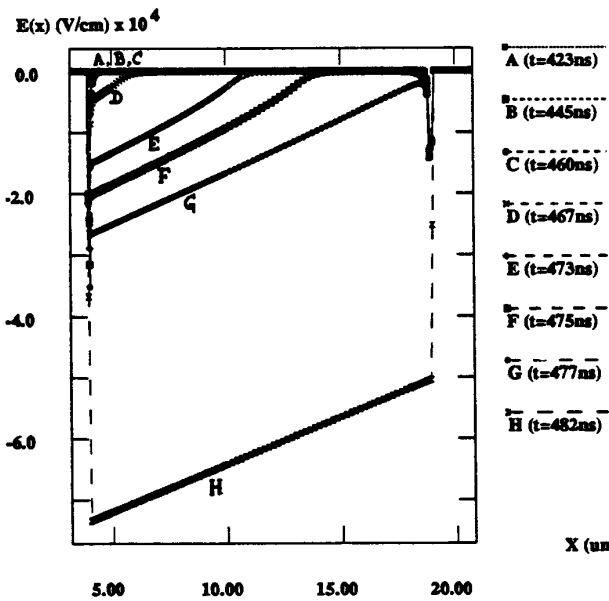


Figure 4: Electric field as a function of time

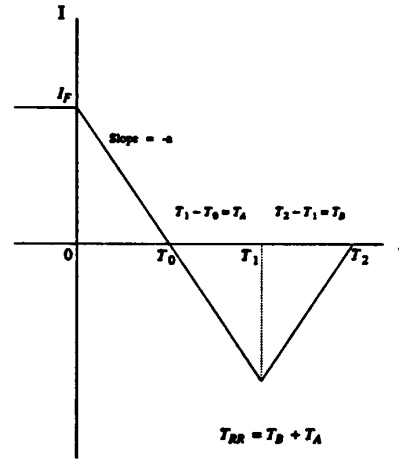


Figure 5: An idealized reverse recovery waveform. The various time instants are also illustrated

III. Determination of Carrier Lifetimes

The technique for determining lifetime is based on a charge-control analysis, i.e.,

$$\frac{dQ(t)}{dt} = -\frac{Q(t)}{\tau} + I(t) \quad (1)$$

This analysis is different from that of [1] in that the "snappiness" of the turnoff is taken into account. For the time interval $0 < t < T_1$, the charge as a function of time is given by (2)

$$Q(t) = a\tau(T_0 - \tau - \tau e^{-t/\tau}) \quad (2)$$

For $T_1 < t < T_2$, the current increases at a rate of a/S , and

$$Q(t) = \frac{a\tau}{S} \left((t - T_1 - \tau) - ST_A + e^{-(t-T_2)/\tau} \right) \quad (3)$$

From (2) and (3), an implicit relation for the lifetime τ can be obtained as

$$e^{T_B/\tau} = 1 + S - S e^{-T_1/\tau} \quad (4)$$

In the special case $T_1 \gg \tau$, (4) gives,

$$\tau = T_B / \ln(1 + S) \approx T_B \sqrt{1 + S} / S = \sqrt{T_A T_{RR}} \quad (5)$$

The lifetime can then be determined as $\tau \approx \sqrt{T_A T_{RR}}$.

The above technique for determining lifetime is verified using simulations from CODECS. Different values of lifetimes were chosen for the rectifier under simulation and compared with lifetimes extracted from the reverse-recovery measurements. In Fig. 6, the lifetimes determined from (5) are plotted for different W , the length of the i-region. The listed high-level injection lifetimes are the sum of the low-level injection lifetimes [2]. A single value of lifetime is obtained, which is in agreement with the high-level injection lifetimes used in the simulations.

Experimental reverse recovery waveforms obtained from a 490V and a 200V p-i-n rectifier are shown in Fig. 7. In one case I_F is kept fixed and the ramp rate is varied, whereas in the second case I_F is varied with a fixed ramp rate. The lifetime values extracted from the measured devices are plotted as a function

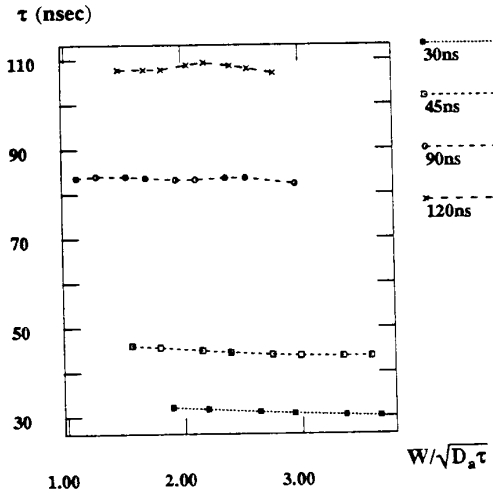


Figure 6: Lifetime values extracted from simulated results plotted against $W/\sqrt{D_a\tau}$ where D_a is the ambipolar diffusion constant. The extracted values are insensitive to W and are in good agreement with the high-level injection lifetimes used in the simulations and listed above.

of T_0 , in Fig. 8. Since each set of waveforms are taken on one device, only one lifetime will be obtained from Fig. 7(a) and another from Fig. 7(b), as seen to be the case in Fig. 8. The lifetimes for these examples are determined by use of (4).

Simulations have verified that T_A and T_B are independent of I_F and dI/dt for $T_1 \gg \tau$. Experimental data provides additional confirmation as shown in Fig. 9. It is seen that although, I_F and dI/dt are varied T_A , T_B and S remain constant.

IV. Modeling of Softness Factor

The factors that affect S can be understood by studying the dependence of T_A and T_B on W and τ .

In Fig. 10 simulated T_A is plotted as a function of τ , with W as a parameter. Fig. 11 shows the corresponding dependencies of T_B . It can be seen from Fig. 10 that T_A can be fit as $T_A = k(W)\tau$, where $k(W) \leq 1$ is a weak function of W . The dependence of T_B on W and τ is hard to model analytically and, therefore, simulations are necessary for determining S . The simulated value of S is shown in Fig. 12. It can be seen that in the range of W and τ

$$S = -0.3 + 0.315 \ln W - 0.1 \ln \tau \quad (6)$$

Eq. (6) is also plotted in Fig. 12. As W increases or $L_a = \sqrt{D_a\tau}$ decreases, a relatively larger portion of the stored charge remains in the i-region at $t = T_1$. S is related to the time required to exhaust this charge and hence it increases.

V. Effect of Circuit Inductance

In this section the effect of the inductance is examined. Simulations have been performed for different values of L , and a fixed value of $V_R = 10V$. S and the peak reverse voltage as a function

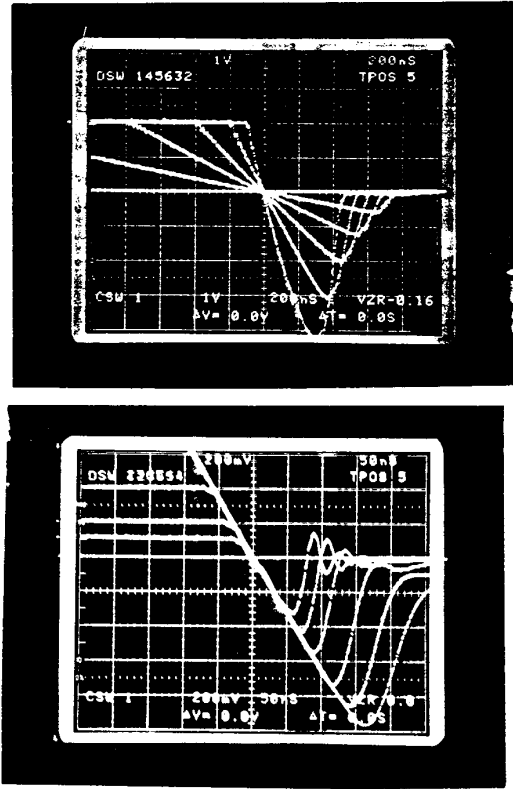


Figure 7: Measurements on experimental devices. (a) I_F is kept constant and dI/dt is varied. (b) I_F is varied and dI/dt is constant.

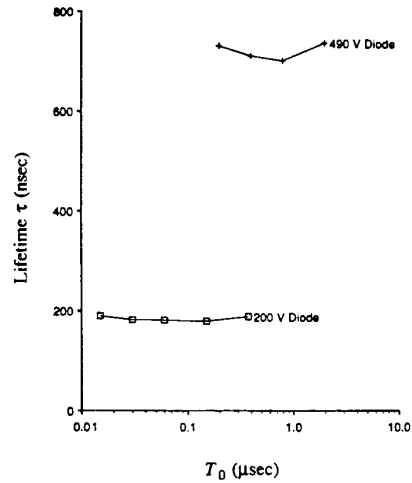


Figure 8: Lifetime values extracted from experimental data

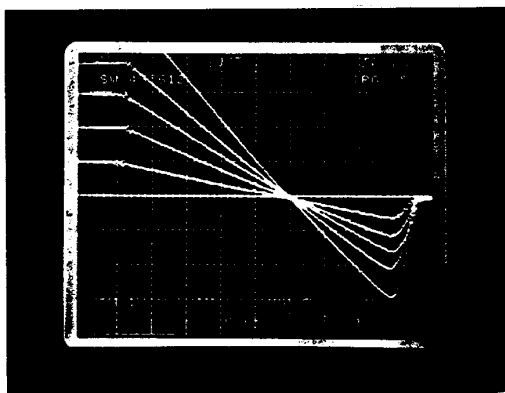


Figure 9: Experimental data indicates that T_A and T_B are independent of dI/dt and I_F for $T_1 \gg \tau$.

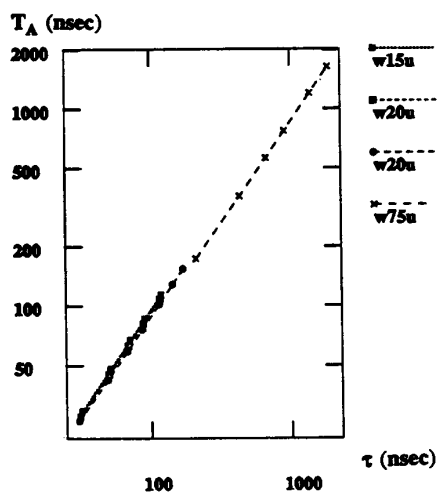


Figure 10: Simulated value of T_A as a function of τ and W

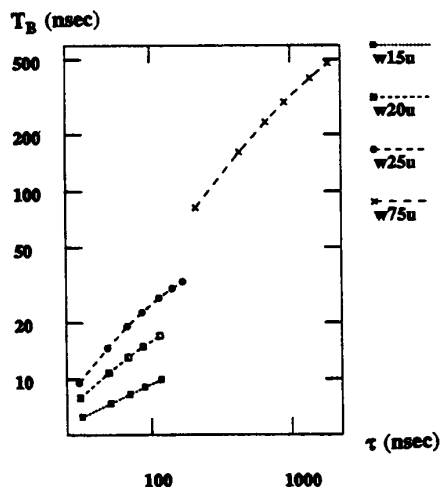


Figure 11: Simulated value of T_B as a function of τ and W

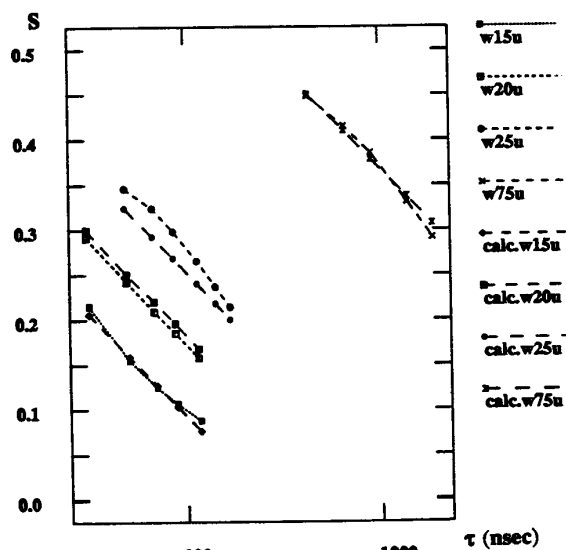


Figure 12: Simulated value of S as a function of τ and W . Also shown are the results from Eq. (6)

of L are given in Table 1. S is seen to have a weak dependence

L (μH)	0.25	0.40	0.50	0.60	0.80	1.00
S	0.196	0.206	0.215	0.224	0.240	0.257
V_P (Volts)	133.5	110.7	101.0	94.0	83.7	76.7

Table 1: S and V_P dependence on L

on L . A smaller L results in a proportionally larger dI/dt during T_A , and even larger dI/dt during T_B due to the decreasing S . Hence, larger reverse-voltage spikes are obtained for smaller L 's.

VI. Conclusions

Power devices in arbitrary RLC circuits can be simulated with the coupled device and circuit simulator CODECS. Simulations and experiments have been used to verify a technique for determining high-level injection carrier lifetime. The softness factor is difficult to model and simulations provide a useful means for evaluating the effect of τ and W on S ; $S \approx -0.3 + 0.315 \ln W - 0.1 \ln \tau$. Softness can be increased by increasing W/L_a subject to the forward voltage trade-off.

Acknowledgements

This research is supported by SRC grant number 82-11-008 and by General Electric Company under the MICRO program.

References

- [1] Y. C. Kao and J. R. Davis, *IEEE Trans. Electron Devices*, pp. 652-657, Sept. 1970.
- [2] S. K. Gandhi, *Power Semiconductor Devices*, John Wiley and Sons, 1977.